Journal of Petroleum Science and Engineering 172 (2019) 1103–1111

Contents lists available at ScienceDirect

Journal of Petroleum Science and Engineering

journal homepage: www.elsevier.com/locate/petrol

Time series data analysis for automatic flow influx detection during drilling

Hewei Tang[a], Shang Zhang[b], Feifei Zhang[c,d,*,1], Suresh Venugopal[d]

[a] Texas A&M University, United States
[b] The University of Tulsa, United States
[c] Yangtze University, China
[d] Halliburton, United States

ARTICLE INFO

Keywords:
Kick detection
Time series data
Automatic detection
Offshore drilling
Dimensionless kick indicators

ABSTRACT

Automatic and early detection of flow influx during drilling is important for improving well-control safety. In this paper, a new method that can automatically analyze real-time drilling data and detect the flow influx event is presented. The new method combines the physics-based dimension reduction and time-series data mining approaches. Two kick indicators are defined, representing the drilling parameter group (DPG) and flow parameter group (FPG), respectively. Additionally, two real-time trend-analysis methods, the divergence of moving average (DMA), and the divergence of moving slope average (DMSA) are applied to quantify trend evolutions of the two indicators. The kick event is identified based on the anomalous trends held by the two kick indicators. A final kick-risk index (KRI) is calculated in real time to indicate the probability of kick events and to trigger the alarm. The method is tested against four offshore kick events. With KRI threshold setting as 0.8, the average detection time is 64% less than the reported detection time. The application of DPG kick indicator allows the early kick detection without additional downhole sensors or costly flow meters.

1. Introduction

Flow influx during drilling is an undesired and uncontrolled influx of formation fluid into the wellbore when the formation pore pressure is higher than the wellbore pressure, which is also known as “kick.” If the kick is not detected and controlled in time, it can potentially result in a blow-out event, which can result in injury or loss of life. The blow-out event can also be harmful to the environment and cost the company billions of dollars.

Even though the kick is controlled before a blowout occurs, the time taken for drilling engineers to detect the problem and take action can make a huge difference. According to Phil Griffin (1967), the maximum killing pressure required will be more than two times higher if the kick is detected 15 min later. Therefore, it is crucial that the kick event is detected as early as possible to reduce the difficulties of well control and non-productive time (NPT) on the drilling rig.

The flow influx during drilling is primarily detected by observing the difference of mud-return flow rate and flow-in rate (delta flow) or mud-pit volume changes (Brakel et al., 2015). A kick is detected when the return flow rate is greater than the flow-in rate or when there is an increase in the mud pit level. The measurement of the mud-return flow rate highly depends on the quality of flow sensors, especially for offshore drilling. However, accurate flow meters, such as the Coriolis flow meter, are costly and are not commonly applied. Commonly applied sensors, such as flow paddles, are not very accurate and can often get stuck. In addition to flow influx, other operating factors, such as changing the pits and increasing the drilling fluid can also result in a mud-pit gain. These factors make pit volume changes even less applicable than the delta-flow (Pournazari et al., 2015). Furthermore, both delta flow and mud-pit level are detected on the derrick floor. For deep-water drilling, it can take a much larger amount of time for the kick to be observed on the derrick floor than onshore drilling.

Standpipe pressure is often chosen as a second kick indicator for rapid kick detection or confirmation (Swanson et al., 1997). However, the detection of additional pressure losses resulting from the flow influx typically relies on detailed hydraulic models. These models require a large number of well parameters as inputs to obtain accurate results. Reitsma (2011) introduced a method of applying standpipe and discharge pressure for rapid kick detection. The method required additional pressure sensors to achieve the detection.

Traditional kick detection methods calculate predicted values of kick indicators and then compare them with the actual values from sensor readings (Cayeux et al., 2014; Swanson et al., 1997). The prediction usually includes solving ordinary differential equations or

* Corresponding author.
E-mail address: feifei-zhang@yangtzeu.edu.cn (F. Zhang).
[1] Previously with Halliburton, now with Yangtze University, China.

https://doi.org/10.1016/j.petrol.2018.09.018
Received 10 June 2018; Received in revised form 29 July 2018; Accepted 4 September 2018
Available online 07 September 2018
0920-4105/

partial differential equations, which requires high computational power for real-time modeling and analysis. Statistical-analysis-based methods have recently become popular in automatic drilling hazard alerting systems (Mickens et al., 2017; Pournazari et al., 2015; Salminen et al., 2017; Tarr et al., 2016). These methods often require less computational cost and have no limitations on physical application scope, as compared to traditional physical-based methods. Real-time drilling data are a time-series data stream by nature. Because of the continuous nature of time series, it is always analyzed as a whole, rather than by individual numeric fields (Fu, 2011). Pournazari et al. (2015) applied a symbolic aggregate approximation (SAX) method to convert the real-time drilling data to symbolic string for kick detection. The method can efficiently reduce the dimension of the original data. Tarr et al. (2016) applied different pattern-recognition methods for kick detection during connections. They found an upper limit of 800 s to capture all pumps-off transient flow patterns. However, this limit value is difficult to apply in kick detection during drilling, especially considering that flow paddles can occasionally malfunction. Sun et al. (2018) proposed a pattern recognition model for gas kick detection in offshore drilling. The analysis was based on four kick indicators: outflow rate, pit gain, standpipe pressure and rate of penetration. However, our analysis on the available offshore data indicated that one can hardly confirm a kick event only based on the four kick indicators mentioned above.

The objective of this paper is to develop a novel statistical-analysis-based kick detection method for real-time drilling data. The method is required to consider the uncertainties of actual field data, which include fluctuations, outliers, and the malfunctions of flow meters. In this method, a new kick indicator is proposed for early kick detection. The kick indicator integrates several drilling parameters to enable earlier kick detection. Furthermore, a time-series analysis algorithm is introduced for automatic anomalous trend detection in real time. A workflow for automatic early kick detection from real-time drilling data is also presented. Finally, the actual drilling data from multiple offshore rigs are applied to demonstrate the capability of this new early kick detection method.

2. The new kick indicator

Traditional kick indicators include delta flow increase (flow-out rate > flow-in rate), drilling break (ROP sudden increase), weight-on-bit (WOB) decrease, standpipe pressure (SPP) decrease, and torque increase. To identify a kick event, a drilling engineer must monitor several parameters at the same time. One can miss important warning signs, especially when most indicators provide little information and, sometimes, even contradict trends. A lot of field experience is required to identify a kick in field operations.

In the proposed method, the normalized rate of penetration (also known as d-exponent) is used as the main indicator for early kick detection. Jorden and Shirley (1966) first introduced the concept of the d-exponent. As shown in Eq. (1), the d-exponent lumps together the following drilling parameters: rate of penetration (*ROP*, in ft/h), rotary speed (*N*, in RPM), weight on bit (*WOB*, in lbf) and bit size (D_{bit}).

$$d = \frac{\log\left(\frac{ROP}{60N}\right)}{\log\left(\frac{12WOB}{10^6 D_{bit}}\right)} \tag{1}$$

The d-exponent has been applied in the oil and gas industry for identifying abnormal pressure formation and detecting abnormal pore pressure. In normal-pressured formations, the d-exponent follows an increasing trend. When the drilling bit encounters over-pressured formations, the d-exponent will deviate from the original increasing trends and follow a slower increasing or decreasing trend (Serebryakov et al., 2002). Fig. 1 illustrates how the d-exponent is applied in abnormal formation pressure identification. The transition between normal pressure formation and abnormal pressure formation can be immediately detected by the d-exponent through the deviation from normal trends. Therefore, the d-exponent can be used as a real-time indicator for encountering abnormal pressure formations. The d-exponent is, thus, a good indicator for kick detection because most of the kicks during drilling occur at a time when the well is penetrating through over-pressured zones. The advantages of applying the d-exponent are that no additional sensors are required, the impact of operating parameter changes can be reduced, and the detection can still work even if the flow meter malfunctions.

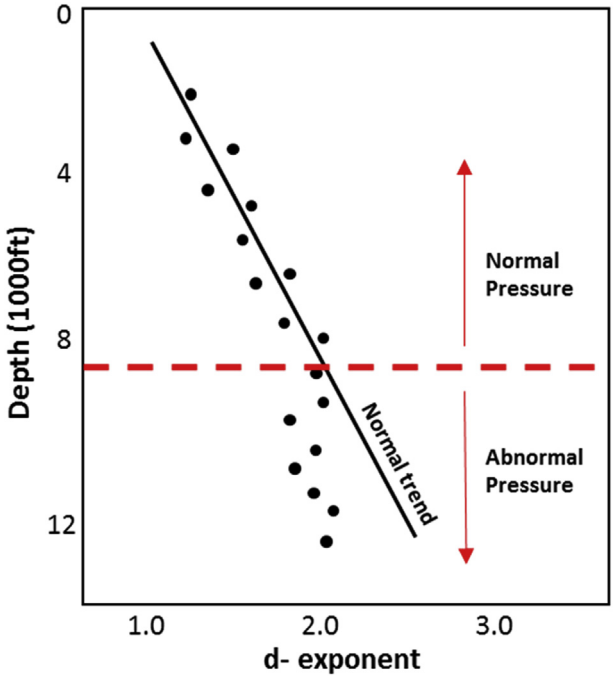

Fig. 1. Illustration of d-exponent for abnormal pressure formation identification during drilling (modified from Fertl et al., 2002).

Because the d-exponent groups together several important drilling parameters for kick detection, we will refer to it as the drilling parameter group (DPG) in the following sections. Note that DPG can also be applied to slide drilling mode; thus, the same set of operational parameters from the rotary motor can be used to conduct the calculation. For example, the RPM used for the calculation during slide drilling mode should be the RPM of the mud motor instead of the RPM of the entire drilling string. The WOB calculation is also different from rotatory drilling because the frictional loss on the drilling string would be larger at stationary mode. Johancsik et al. (1984) presented details about the calculation of drilling string mechanics.

Similarly, a flow parameter group (FPG) lumps together the flow out rate (*FlowOut*), the flow in rate (*FlowIn*) and the standpipe pressure (*SPP*) is defined by Eq. (2):

$$FPG = Flow\ Out\ - \frac{Flow\ In}{1\ - c_r \times (SPP - P_{ref})} \tag{2}$$

where, c_r is the compressibility of the drilling mud and P_{ref} is the reference pressure (14.7 psig). The physical meaning for FPG is the pressure-calibrated flow gain, which is mainly influenced by the drilling fluid density and formation pressure. When kick occurs, FPG will tend to increase, indicating that flow-out rate is increasing compared to the flow-in rate. DPG and FPG are applied as two major kick indicators for this new kick detection method.

3. Detection of anomalous trends in real-time drilling data

There are two challenges associated with the automatic detection of anomalous trends in real-time drilling data. The first is to quantify the

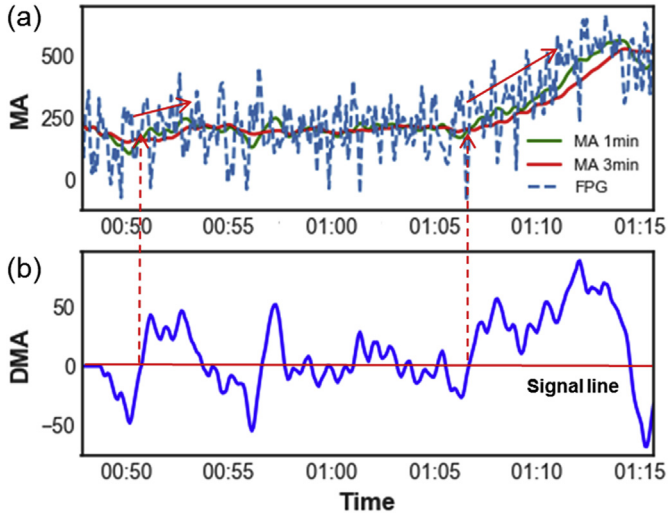

Fig. 2. (a) Original FPG data and average FPG values with window sizes of 1 min and 3 min. (b) The calculated DMA data with the zero DMA value represented as a signal line.

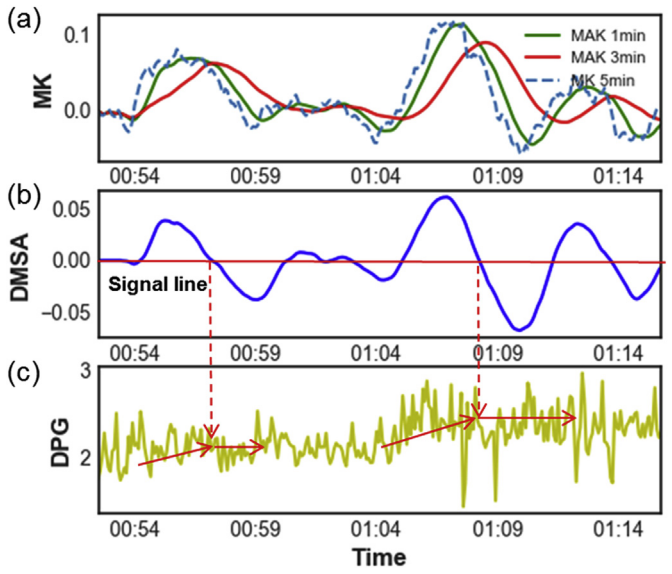

Fig. 3. (a) The moving slope value (MK) of DPG data and moving averages of the moving slope value (MAK) with window sizes of 1 min and 3 min. (b) The calculated DMSA data with the zero DMSA value as a signal line. (c) Original DPG data.

trend in real time. The second is to distinguish the local fluctuations from the long-term trend.

3.1. Trend quantification for time-series data

For the increasing trend shown by FPG, a divergence of moving average value (DMA) is introduced, as shown in Eq. (3).

$$DMA_t = MA_{\alpha,t} - MA_{\beta,t}\ (\alpha < \beta) \tag{3}$$

$MA_{\alpha,t}$ and $MA_{\beta,t}$ are moving average values at time, t, with a sliding window length of α and β, respectively. The algorithm is based on the observation that the shorter sliding window's averages move faster than the longer ones (Zhang et al., 2009). The DMA value is positive when the shorter window average is above the longer window average, which indicates an increasing trend. On the contrary, the negative DMA value represents a decreasing trend. Fig. 2 presents an example of real-time FPG. Average FPG values with window sizes of 1 min and 3 min are first

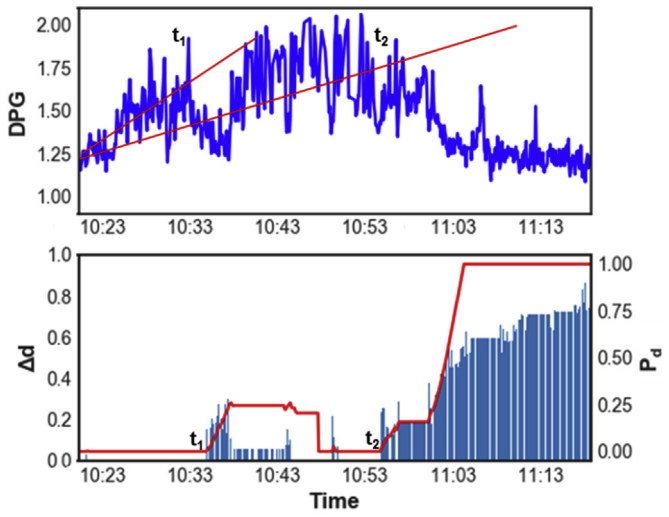

Fig. 4. (a) Original DPG data with regression lines generated at times, t_1 and t_2. (b) The calculated Δd values and P_d values.

calculated, as shown in Fig. 2a. The DMA values are then obtained as the divergence between MA_{1min} and MA_{3min}, as shown in Fig. 2b. We represent the zero DMA value as a signal line. Whenever the DMA values cross above the signal line, a local increasing trend of the original data can be detected.

The above technique only works for the quantification of increasing and decreasing trends. To quantify the slower increasing trend held by DPG, a new strategy is introduced to quantify the accelerating and decelerating trends. First, a sliding window linear regression is applied to the real-time data, and the slope value of the regression at time t is then recorded as MK_t. The value of MK_t directly represents the local trends of the data, with positive values representing positive trends and negative values representing negative trends. A weighted moving average algorithm as shown in Eqs. (4) and (5) is applied to calculate the average local slopes (MAK_t). The algorithm allows for a convenient real-time calculation of the divergence between two moving slope averages, as shown in Eq. (6).

$$w_{i,t} = \frac{1}{1 + \exp\left[-2\frac{i - \lambda_1 - t}{\lambda_2}\right]} \tag{4}$$

$$MAK_t = \frac{\sum_{i=1}^{t} w_{i,t} \times MK_{i,t}}{\sum_{i=1}^{t} w_{i,t}} \tag{5}$$

$$DMSA_t = MAK_{\alpha,t} - MAK_{\beta,t}\ (\alpha < \beta) \tag{6}$$

In Eq. (4), $w_{i,t}$ is the weighting factor for data points i before time step t. $MAK_{\alpha,t}$ and $MAK_{\beta,t}$ are the average local slops (MAK_t) with sliding window lengths of α and β, respectively. Eq. (4) is a logistic function representing the exponential transition from 0 to 1. λ_1 and λ_2 separately controls the location and the sharpness of the transition respectively. For $\lambda_1 = 0.5 - \alpha$ and $\lambda_2 = 0.1$, weighting factors are close to zero for $i \le t - \alpha$ and close to one for $t - \alpha < i \le t$. $DMSA_t$ is the divergence moving slope average values at time step, t. Positive $DMSA_t$ values represent accelerating trends of the time-series data, and negative $DMSA_t$ values represent decelerating trends. Fig. 3 applies real-time DPG data as an example to illustrate the above process. The MK value of DPG is first calculated with a sliding window size of 5 min. The DMSA value is then obtained by calculating the difference between MAK_{1min} and MAK_{3min}. Similar to the analysis on DMA, DMSA value is negative when the shorter window average (MAK_{1min}) is below the longer window average (MAK_{3min}), which indicates a decreasing trend of local slops. Therefore, we apply the zero DMSA value as a signal line.

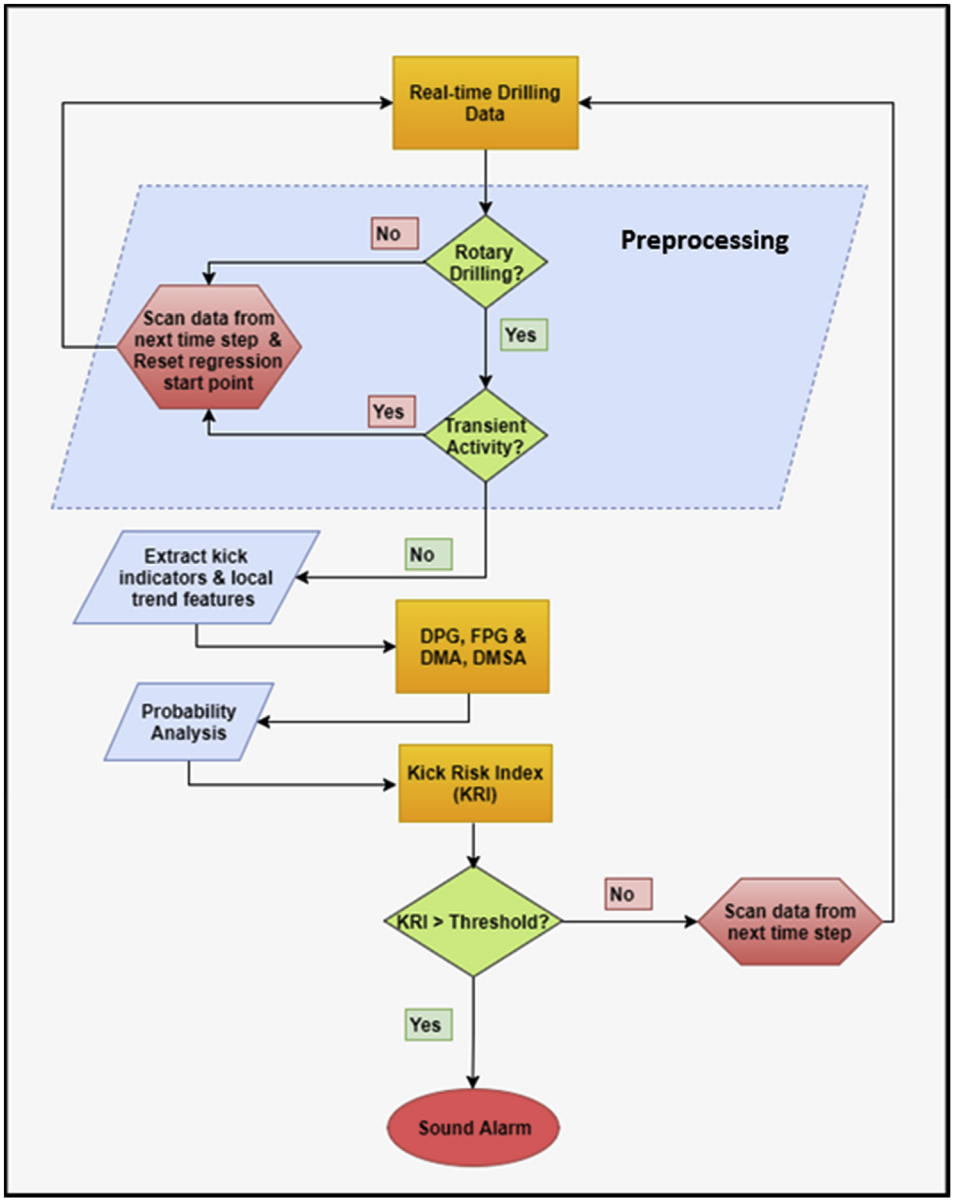

Fig. 5. Flowchart of the new automatic kick detection method.

Table 1
Input conditions of four kick cases.

Case Number	Sliding Window (Short)	Sliding Window (long)	DPG Tolerance	FPG Tolerance	DPG Weighting Factor	FPG Weighting Factor
1	1 min	3 min	0.5	400 gal	0.5	0.5
2	1 min	3 min	2	400 gal	0.7	0.3
3	1 min	3 min	2	100 gal	0.9	0.1
4	1 min	3 min	0.5	200 gal	0.7	0.3

Whenever the DMSA values cross below the signal line, a local slower increasing or decreasing trend can be detected.

3.2. Probability analysis

Another challenge associated with the automatic abnormal trend detection is distinguishing the local fluctuations from long-term trends. As shown in Fig. 4a, the DPG value follows an increasing trend from 10:23am to 10:53am and then changes to a decreasing trend because the drilling bit encounters an over-pressured formation. A local decreasing trend, which is a local fluctuation and could potentially lead to false alarms, is ignored at around 10:35am in the above analysis. For real-time detection, it is difficult to confirm that the decreasing trend at 10:35am is a local fluctuation until the data change back to their original increasing trend at around 10:45am. Therefore, a probability analysis algorithm is introduced to make the above visual detection process automatic and quantified.

The algorithm is based on the transaction signals given by the DMSA values. The DPG data set shown in Fig. 4 is applied as an example. Whenever a local decreasing trend is detected, predictions based on the

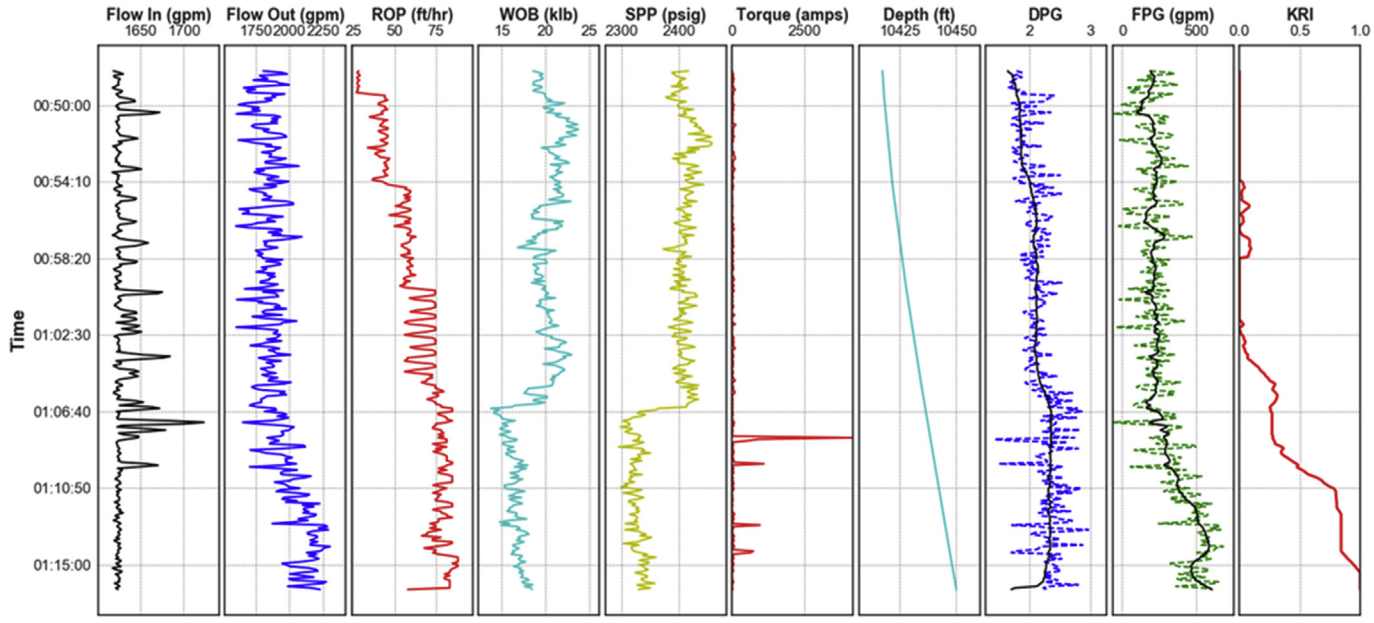

Fig. 6. Real-time drilling data and calculated DPG, FPG, and KRI values of case 1.

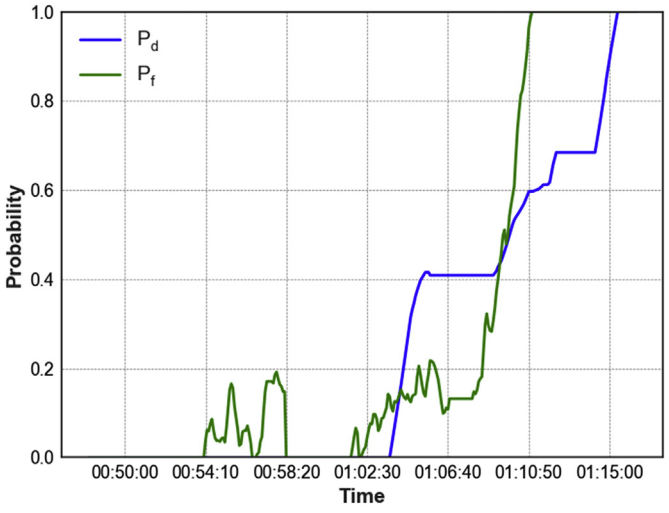

Fig. 7. Probability analysis results of DPG and FPG for case 1.

linear regression of previous DPG data will be calculated, as shown for times t_1 and t_2 in Fig. 4a. The difference of predicted DPG values and actual DPG values make up the Δd histograms shown in Fig. 4b. A deviated area (D_{area}) is calculated by integrating the Δd histograms with time, as shown in Eq. (7). A DPG probability (P_d) is further obtained by dividing the D_{area} with a specific tolerance value ($D_{tolerance}$), as shown in Eq. (8). Fig. 4b shows the final calculated value of P_d with a tolerance value of 2.

$$D_{area} = \int (DPG_{pred} - DPG_{actual})dt \tag{7}$$

$$P_d = \frac{D_{area}}{D_{tolerance}} \tag{8}$$

Similarly, a FPG probability (P_f) can be calculated through Eqs. (9) and (10) with a specific tolerance value ($F_{tolerance}$).

$$F_{area} = \int (FPG_{actual} - FPG_{pred})dt \tag{9}$$

$$P_f = \frac{F_{area}}{F_{tolerance}} \tag{10}$$

F_{area} and $F_{tolerance}$ have a physical meaning of pit-volume gain. For the above calculations, the probability value is made to be 1 if the value of the deviated area is larger than the tolerance values.

A final kick risk index (*KRI*) can be calculated by assigning different weighting factors (w_d and w_f) to DPG probability and FPG probability as shown in Eqs. (11) and (12). The KRI value is between 0 and 1, and it indicates the probability of kick events.

$$KRI = w_d P_d + w_f P_f \tag{11}$$

$$w_d + w_f = 1 \tag{12}$$

4. Workflow of automatic kick detection

The flowchart of the new automatic kick detection algorithm is presented in Fig. 5. As shown in the flowchart, the real-time drilling data is read into the algorithm time step by time step. The algorithm first evaluates whether the data belongs to the rotary drilling process or non-drilling process (e.g., tripping, reaming, or workover). By preprocessing the real-time data, the data goes through a series of checks before loading into the kick detection algorithm. Those checks evaluate the real-time data based on physical indicators of the drilling operation, such as ROP, WOB, torque, pump activities, well depth, and drill-bit locations. Once a rotary drilling process is confirmed, the algorithm then checks whether the incoming data belong to any operational transient activities, such as pump rate changes or chock-line operations. The above preprocessing process can help us set up a reasonable starting point for the subsequent probability analysis, as well as avoid false alarms caused by transient events. Then, kick indicators (DPG and FPG) and local trend features (DMA and DMSA) are calculated based on data at current and previous time steps. Probability analysis is further conducted if the DMA value indicates a local increasing trend or if the DMSA value indicates a local slower increasing or decreasing trend. A final kick risk index can be obtained by assigning different weighting factors to DPG and FPG indicators. In this study, the kick alarm threshold is set at 0.8. An alarming signal will be given by the algorithm if the KRI value is larger than 0.8.

5. Case studies

Real-time drilling data from multiple offshore deviated wells are

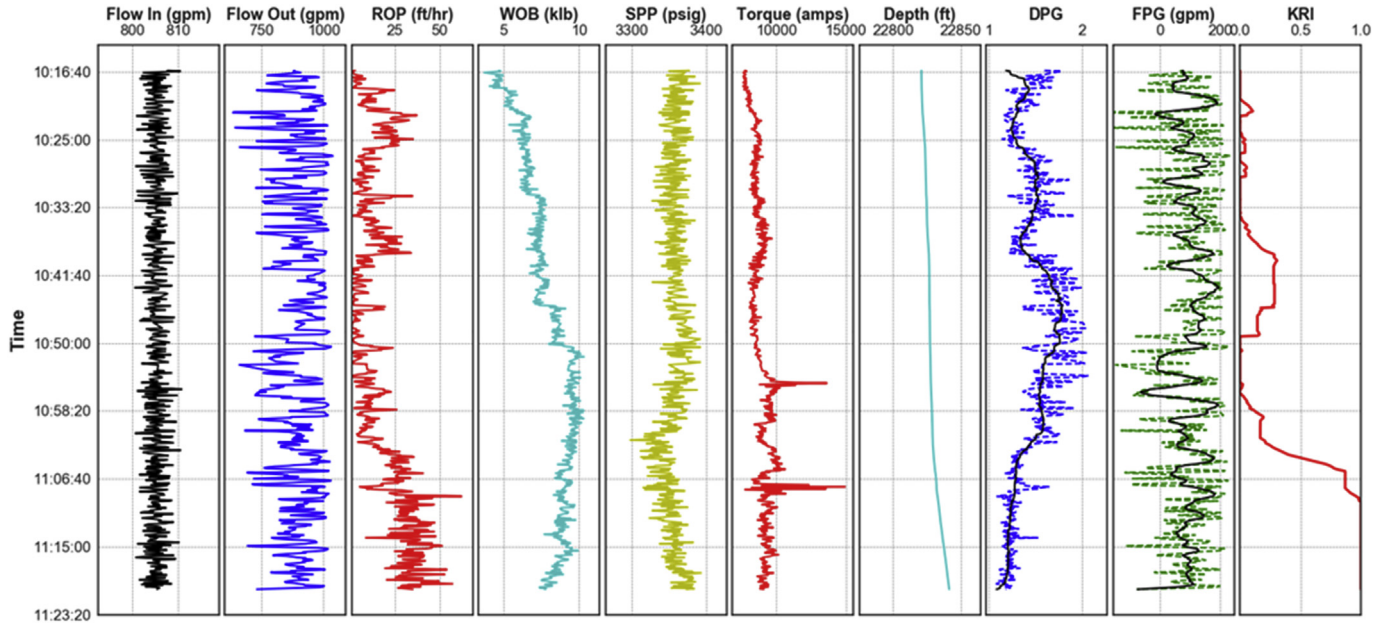

Fig. 8. Real-time drilling data and calculated DPG, FPG, and KRI values of case 2.

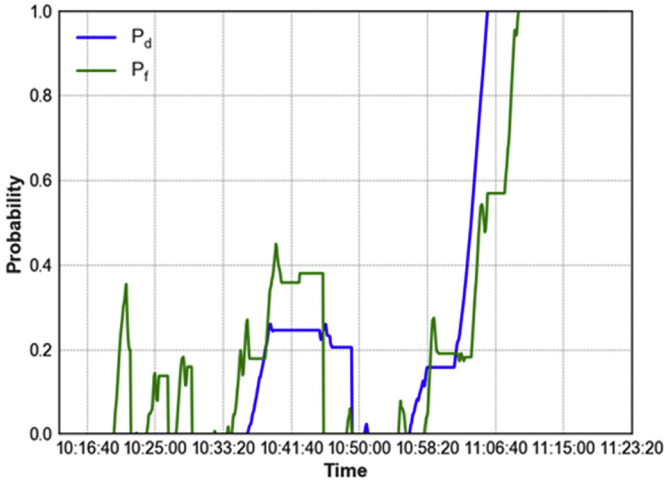

Fig. 9. Probability analysis results of DPG and FPG for case 2.

applied to test the reliability of the new algorithm. In this section, the testing results of four reported kick events are presented. In Case 1, both DPG and FPG show obvious abnormal trends when kick occurs. In Case 2, DPG shows an obvious deviation from the normal trend, while the deviation of FPG cannot be easily observed. In Case 3, FPG is not applicable, but DPG still functions well. In case 4, although the trend information in FPG is not clearly shown, it helps avoid a potential false alarm from DPG. The input conditions of each case are summarized in Table 1. The influence of different input conditions on the kick detection results will be discussed in the next section.

5.1. Case 1

A period of 30-min real-time drilling data is shown in Fig. 6. The data was recorded every 5 s. Tracks 1 through 6 present traditional kick indicators, such as flow-in/out rate, ROP, WOB, SPP and torque. Track 7 shows the measured depth (MD). Tracks 8 and 9 present the new kick indicators of DPG and FPG. Dash lines represent the original data. Solid black lines are the smoothed data through the application of a median filter with a kernel size of 51. Track 10 presents the calculated kick risk index (KRI).

From the drilling report, a kick of 17-bbl influx fluid was detected at around 01:17, when the drilling bit reached 10,450 ft MD. The well was shut and the kick was then circulated out through the chock line. Traditional kick indicators generally work well for detecting this kick event. An obvious flow-out rate increase could be observed at around 01:07. The sudden decreasing trends of ROP, WOB and SPP also increase the certainty of the kick occurrence. Although the torque measurement fails in this case, it does not influence the confirmation of this kick event. As shown in the figure, DPG starts to deviate from its normal increasing trend at around 01:06. FPG starts to show an upward trend at around 01:07, which is slightly slower than the DPG indicator. Fig. 7 shows the calculated DPG probability and FPG probability. The relevant tolerance values for DPG and FPG are 0.5 and 400 gal, respectively. A weighting factor group of 0.5/0.5 is applied to calculate the final KRI. The new algorithm can detect the kick at around 01:10, which is 7 min earlier than the reported detection.

5.2. Case 2

Fig. 8 shows the real-time data of a 60-min drilling period. The data was recorded every 5 s. From the drilling report, the drilling crew observed a 10-bbl gain when drilled to 22,847 ft MD. The drilling crew then flow-checked the well. The well was flowing and was then shut in. The flow-out rate data fluctuated violently, and no obvious increasing trend could be observed. Other traditional kick indicators function well in this case. ROP increases suddenly at around 11:02. WOB and SPP show a decreasing trend at the same time. Torque also increases at around 10:54. Although no obvious flow gain can be observed, an experienced drilling engineer can possibly confirm this kick event in time. The DPG data exhibit an obvious decreasing trend after 10:52. The calculated DPG and FPG probabilities are shown in Fig. 9. The relevant tolerance values for DPG and FPG are 2 and 400 gal, respectively. We can notice the DPG probability increase due to a local decreasing trend between 10:34am and 10:49am. A corresponding FPG probability increase between 10:33 and 10:43 indicates that this local fluctuation might be a small unreported kick. The algorithm also successfully detects the increasing trend held by FPG after 10:58am, although it is hard to be observed visually. Weighting factors of DPG and FPG are 0.7 and 0.3 respectively. The kick is confirmed at around 11:05am, which is 14 min earlier than the reported detection.

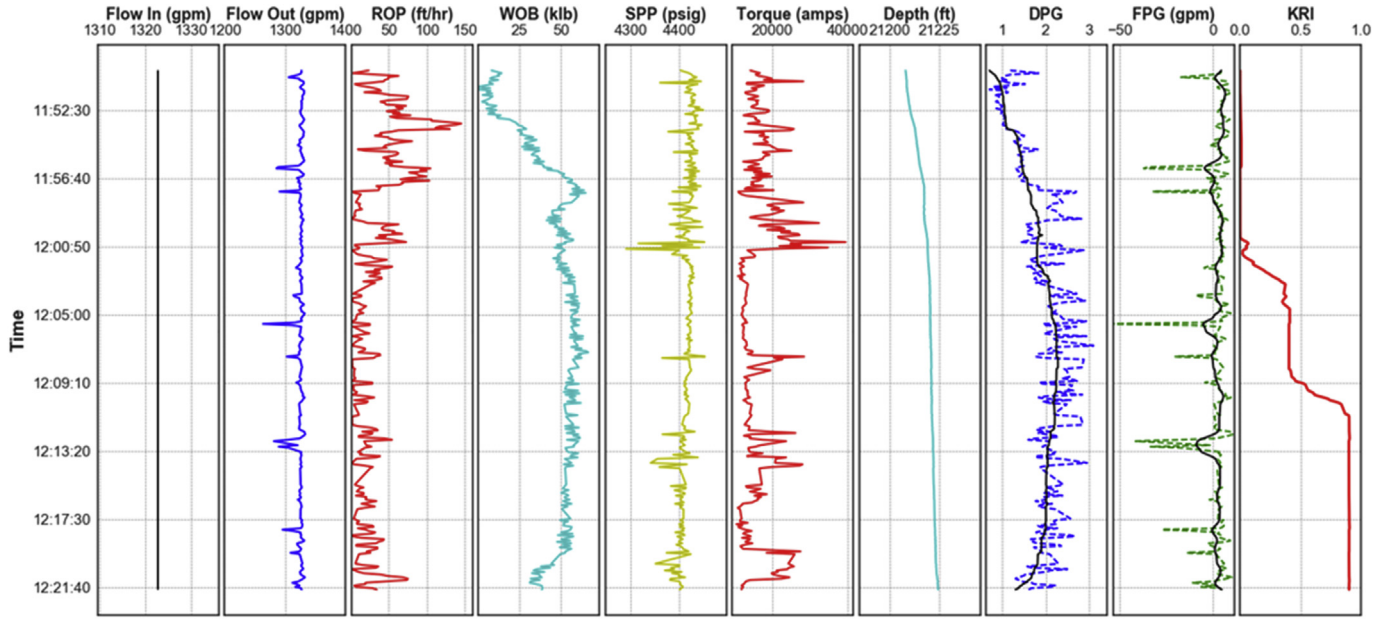

Fig. 10. Real-time drilling data and calculated DPG, FPG, and KRI values of case 3.

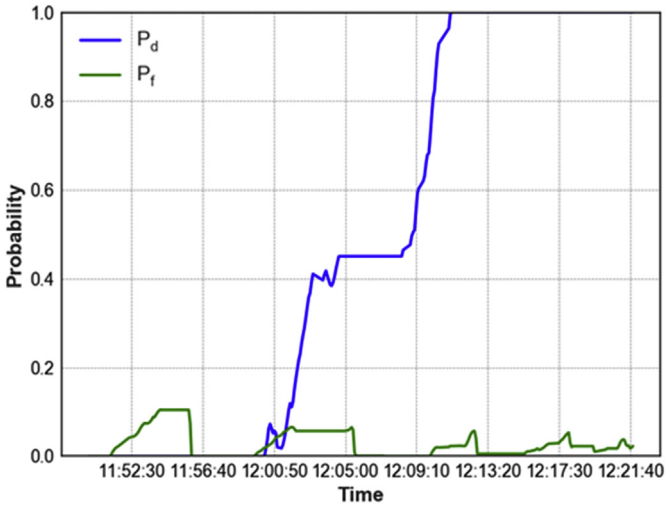

Fig. 11. Probability analysis results of DPG and FPG for case 3.

5.3. Case 3

Fig. 10 shows the real-time data of a 30-min drilling period. The data was recorded every 5 s. The drilling crew observed 11-bbl gain on the system when dilled to 21,224 ft MD at 12:21am. They then picked up and flow-checked the well. This kick event can hardly be identified based on traditional kick indicators. The patterns of flow-in and flow-out rates indicate that the flow paddles were stuck. ROP and torque fail to provide valuable information. WOB and SPP decrease slightly. This kick event is hard to confirm only based on the observation of these traditional kick indicators. However, the new kick indicator, DPG, shows a clear deviation from the normal increasing trend at 12:07pm, which indicates the occurrence of the kick. Fig. 11 presents the calculated DPG and FPG probabilities. The relevant tolerance values for DPG and FPG are 2 and 100 gal, respectively. FPG probability cannot provide any valuable information, because the flow paddle malfunctioned. We give FPG a weighting factor of 0.1 and DPG a weighting factor of 0.9 to calculate the KRI value. The kick-confirmed alarm is set off at 12:11pm, which is 10 min earlier than the reported detection.

5.4. Case 4

Fig. 12 shows the real-time data of a 40-min drilling period. The data was recorded every 1 s. From the drilling report, the drilling crew detected a flow influx at around 18:50 when drilled to 12,075 ft MD. The well was then shut in and well control was applied. Traditional kick indicators do not work well in this case. Flow-out rate fluctuates violently, and no clear increasing trend could be observed. ROP almost stays constant and WOB changes seasonally. SPP decreases throughout the period, which is hard to identify whether the trend is caused by a kick event. Torque holds an increasing trend after 18:38. With most traditional kick indicators fail to provide valuable information, this kick event is also hard to confirm. The calculated DPG also have several fluctuations owing to the seasonal trend of WOB. With much smaller fluctuation amplitude, the deviation trend of DPG is obvious at 18:37. Fig. 13 shows the calculated DPG probability with a threshold of 0.5 and the calculated FPG probability with a threshold of 200 gal. The final KRI is calculated by applying a weighting factor of 0.7 for DPG and a weighting factor of 0.3 for FPG. Notice that we might have a false alert between 18:23 and 18:30 if we purely rely on the DPG indicator. The new algorithm confirms the kick at around 18:41, which is 9 min earlier than the reported detection.

5.5. Case summary

Kick events are difficult to detect in the last three cases only based on the traditional kick indicators, especially when the flow meter is stuck in the third case. The DPG kick indicator introduced by the new method shows clear deviations from the normal trends when kick occurs in all the four cases. In addition, the new method integrates all the information into a real-time kick-risk index (KRI), which provides drilling engineers with more straightforward guidelines to the occurrence of kick events. Table 2 summarizes kick occurrence time, field detection time, and detection time of the new method for the four testing cases. The kick occurrence time is estimated by the time that DPG deviates from the previous increasing trends. The new algorithm can achieve a detection time of 10 min earlier on average. An improved percentage is calculated by dividing the improved time with the difference between the field detection time and the kick occurrence time, representing the percentage of the kick detection time improvement. The algorithm can reduce the kick detection time by 64% on average.

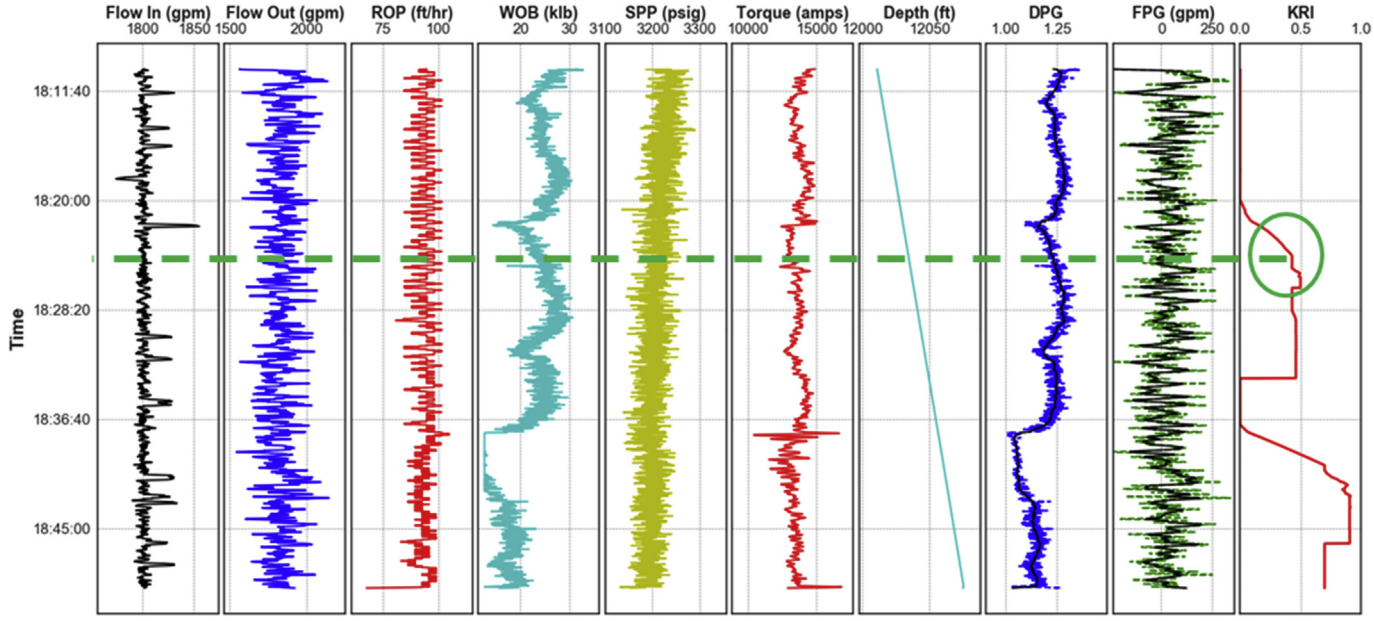

Fig. 12. Real-time drilling data and calculated DPG, FPG, and KRI values of case 4.

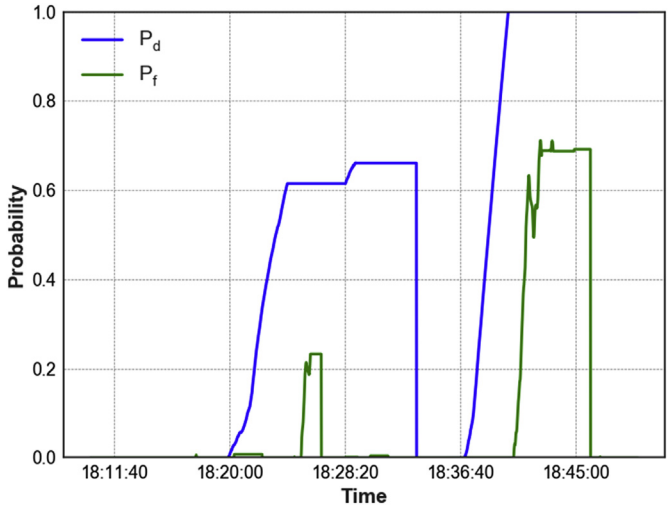

Fig. 13. Probability analysis results of DPG and FPG for case 4.

Table 2
Summary of kick cases.

Case Number	Kick Occurrence	Field Detection	This Method	Improved Time	Improved Percentage
1	01:06	01:17	01:10	7min	63.6%
2	10:52	11:19	11:05	14min	51.9%
3	12:07	12:21	12:11	10min	71.4%
4	18:37	18:50	18:41	9min	69.2%

6. Discussion

In the above algorithm, four categories of parameters can influence the detection time of kick events: kick alarm threshold for KRI value, sliding window size for DMA and DMSA calculations, tolerance values, and weighting factors for DPG and FPG kick indicators. A low kick-alarm threshold leads to early kick detection, but it can also increase the risk of false alarms. Parametric studies are conducted to investigate the influence of each parameter on the final results, which are summarized in Table 3. Row No. 1 presents the relevant parameters and improved time for Case 2, which is served as the base case. Rows No. 2 through 4 present the results of different sliding window sizes. It can be concluded that a larger difference between the short sliding window and long sliding window might delay the detection (No. 2), while a smaller difference might lead to an earlier detection (No.4). The time delayed or earlier is totally based on the time difference of sliding windows. For all the cases in the result section, a universal short window size of 1 min and a long window size of 3 min are applied. Rows No.5 through 7 present the results of different tolerance values. If the tolerance value of DPG is decreased to 0.5, the kick can be detected 2 min earlier than the base case. The trade-off is that the algorithm gives a false alarm at around 10:38. Similarly, if the tolerance value of FPG is decreased, the algorithm can achieve earlier detection, as shown in rows No. 6 and 7. If the FPG is given more weighting, a false alarm will also be set out because of the smaller tolerance value (No. 7). Early detection and accurate detection is always a trade-off problem with regard to tolerance values of kick indicators and kick alarm threshold. Results in row No. 8 indicate the effect of weighting factors between DPG and FPG. Increasing the weighting factor of FPG to 0.7 will lead to a 3-min delay in detection time.

Through the field data testing, it is found that the performance of the DPG indicator is generally better than the FPG indicators in aspects of robustness and detection speed, as the DPG is calculated from drilling parameters measured near drilling bits, while the FPG is calculated from flow parameters measured on derrick floors. It always takes time for the kick to have impacts on the flow-out rates, especially for offshore drilling rigs.

However, because DPG is an indicator based on the anomalies of ROP and WOB, it is only valid during the penetrating process and cannot be applied to other drilling periods (e.g., circulation, tripping). Other kick indicators, such as FPG, are still needed for the entire drilling process, as well as to improve the confidence of DPG's predictions.

7. Conclusions

This paper introduced a new method for automatic early kick detection by exploiting real-time drilling data. The method effectively reduced the dimension of the drilling data stream into two kick indicators (DPG and FPG). A new parameter, d-exponent, was applied in early kick detection for the first time and resulted in better performance than traditional kick indicators in aspects of robustness and detection

Table 3
Results of parametric studies.

No.	Sliding Window (Short)	Sliding Window (Long)	DPG Tolerance	FPG Tolerance	DPG Weighting Factor	FPG Weighting Factor	Improved Time (min)	False Alarm
1	1 min	3 min	2	400	0.7	0.3	14	No
2	1 min	5 min	2	400	0.7	0.3	13	No
3	0.5 min	3 min	2	400	0.7	0.3	14	No
4	0.5 min	1 min	2	400	0.7	0.3	15	No
5	1 min	3 min	0.5	400	0.7	0.3	16	Yes
6	1 min	3 min	2	100	0.7	0.3	15	No
7	1 min	3 min	2	200	0.3	0.7	15	Yes
8	1 min	3 min	2	400	0.3	0.7	11	No

speed. A new time-series data analysis algorithm was applied to automatically detect the anomalous trends held by the kick indicators in real time. Finally, a kick risk index is calculated to provide straightforward real-time monitoring and alarms for kick events.

The new method was tested with four kick events and showed reliable performance. Kick events were identified, on average, 10 min before the reported detection. The average detection time reduction was 64%. This new early kick detection method can be applied in a real-time rig monitoring system without any high requirements on computational power.

Acknowledgements

The authors would like to thank Halliburton for authorizing the publication of this paper.

Nomenclature

c_r	Compressibility of drilling mud, psi^{-1}
d	D-exponent
D_{area}	Deviated area of DPG
D_{bit}	Bit size
$D_{tolerance}$	Tolerance value for DPG
F_{area}	Deviated area of FPG, gal
$F_{tolerance}$	Tolerance value for FPG, gal
N	Rotary speed, rpm
P_d	Probability of DPG
P_f	Probability of FPG
P_{ref}	Reference pressure, psi
w_d	Weighting factor for DPG
w_f	Weighting factor for FPG
Δd	Absolute difference between predicted values and actual values

Acronyms

DPG	Drilling parameter group
DMA	Divergence of moving average
DMSA	Divergence of moving slope average
FPG	Flow parameter group
MA	Moving average
MAK	Moving average of MK
MK	Moving linear regression slope value
ROP	Rate of penetration
SPP	Stand pipe pressure
WOB	Weight on bit

References

Brakel, J., Tarr, B., Cox, W., et al., 2015. SMART kick detection: first step on the well-control automation journey. SPE Drill. Complet. 30 (03), 233–242. SPE-173052-PA. https://doi.org/10.2118/173052-PA.

Cayeux, E., Daireaux, B., Dvergsnes, E.W., et al., 2014. Toward drilling automation: on the necessity of using sensors that relate to physical models. SPE Drill. Complet. 29 (02), 236–255. SPE-163440-PA. https://doi.org/10.2118/163440-PA.

Fertl, W.H., Chilingar, G.V., Robertson, J.O., 2002. Drilling parameters. Dev. Petrol. Sci. 50, 151–167.

Fu, T.C., 2011. A review on time series data mining. Eng. Appl. Artif. Intell. 24 (1), 164–181.

Griffin, P., 1967. Early kick detection holds kill pressure lower. In: Paper SPE-1755-MS Presented at SPE Mechanical Engineering Aspects of Drilling and Production Symposium, Fort Worth, Texas, 5–7 March, . https://doi.org/10.2118/1755-MS.

Jorden, J.R., Shirley, O.J., 1966. Application of drilling performance data to overpressure detection. J. Petrol. Technol. 18 (11), 1387–1394. SPE-1407-PA. https://doi.org/10.2118/1407-PA.

Johancsik, C.A., Friesen, D.B., Dawson, R., 1984. Torque and drag in directional wells-prediction and measurement. J. Petrol. Technol. 36 (06), 987–992.

Mickens, R., Kumar, D., Smith, G., et al., 2017. Automated trend-based alerting enhances real-time hazard avoidance. In: Paper SPE-184737-MS Presented at SPE/IADC Drilling Conference and Exhibition, . https://doi.org/10.2118/184737-MS.

Pournazari, P., Ashok, P., van Oort, E., et al., 2015. Enhanced kick detection with low-cost rig sensors through automated pattern recognition and real-time sensor calibration. In: Paper SPE-176790-MS Presented at the SPE Middle East Intelligent Oil and Gas Conference and Exhibition, Abu Dhabi, UAE, 15-16 September, . https://doi.org/10.2118/176790-MS.

Reitsma, D., 2011. Development of an automated system for the rapid detection of drilling anomalies using standpipe and discharge pressure. In: Paper SPE-140255-MS Presented at the SPE/IADC Drilling Conference and Exhibition, Amsterdam, The Netherlands, 1–3 March, . https://doi.org/10.2118/140255-MS.

Salminen, K., Cheatham, C., Smith, M., 2017. Stuck-pipe prediction by use of automated real-time modeling and data analysis. SPE Drill. Complet. 32 (03), 184–193.

Serebryakov, V.A., Robertson Jr., J.O., Chilingarian, G.V., 2002. Origin and Prediction of Abnormal Formation Pressures, vol. 50 Gulf Professional Publishing.

Sun, X., Sun, B., Zhang, S., et al., 2018. A new pattern recognition model for gas kick diagnosis in deepwater drilling. J. Petrol. Sci. Eng. 167, 418–425.

Swanson, B.W., Gardner, A.G., Brown, N.P., et al., 1997. Slimhole early kick detection by real-time drilling analysis. SPE Drill. Complet. 12 (01), 27–32.

Tarr, B., Ladendorf, D.W., Sanchez, D., et al., 2016. Next-generation kick detection during connections: influx detection at pumps stop (IDAPS) software. SPE Drill. Complet. 31 (04), 250–260. SPE-178821-PA. https://doi.org/10.2118/178821-PA.

Zhang, C., Weng, N., Chang, J., et al., 2009. Detecting Abnormal Trend Evolution over Multiple Data Streams, vol. 9. pp. 285–296 APWeb/WAIM.